



	<b>Experiment title: SAXS study of the mechanism for the reversible worm-to-sphere transition of thermo-responsive diblock copolymer micelles</b>	<b>Experiment number:</b> SC-3864
<b>Beamline:</b> BM26b	<b>Date of experiment:</b> from: 03/03/2014 to: 07/03/2014	<b>Date of report:</b> 26/08/2015
<b>Shifts:</b> 9	<b>Local contact(s): Giuseppe Portalle</b>	<i>Received at ESRF:</i>
<b>Names and affiliations of applicants (* indicates experimentalists):</b> <b>Dr Lee Fielding*, Dr Nicolas Warren*, Dr Oleksandr Mykhaylyk*, Prof Steve Armes, Ms Charlotte Mable* and Mr Mathew Derry*</b>		

**Report:** Static SAXS and rheo-SAXS measurements were planned for the experiment. Unfortunately, there was no appropriate instrument to perform rheo-SAXS measurements. An attempt was made to collect rheo-SAXS patterns using our home-made Couette cell with aluminium walls but intensity of the scattering was low and unsatisfactory for a further SAXS analysis.

Poly(lauryl methacrylate)-poly(benzyl methacrylate) (PLMA-PBzMA) diblock copolymer spheres, worms or vesicles can be readily prepared via polymerization-induced self-assembly at 20 % w/w solids in *n*-dodecane at 70°C, provided that the mean degree of polymerization of the PLMA stabilizer block is relatively low. The worms form free-standing gels at 20°C, but undergo degelation on heating via a worm-to-sphere order-order transition.<sup>1</sup> Representative static SAXS patterns obtained for PLMA<sub>16</sub>-PBzMA<sub>37</sub> diblock copolymer nano-objects in *n*-dodecane as a function of temperature are shown in Figure 1a. At 20°C, the scattering pattern obtained at 5.0 % w/w copolymer has a negative gradient slightly lower than unity in the low *q* region and also a local minimum in intensity at high *q* ( $\sim 0.50 \text{ nm}^{-1}$ ), indicating a mean worm cross-section of approximately 13 nm. Heating to 160°C leads to a substantial change in this SAXS pattern: the gradient at low *q* tends to zero and the feature at  $q \sim 0.50 \text{ nm}^{-1}$  disappears. On returning to 20°C, a negative gradient at low *q* is again observed (albeit marginally lower than the original gradient) and the minimum at  $q \sim 0.50 \text{ nm}^{-1}$  is almost completely recovered. These observations suggest fairly good reversibility for the worm-to-sphere-to-worm transition over the experimental time scale (hours). In contrast, the same thermal cycle conducted at 1.0 % w/w provides good evidence for the same worm-to-sphere transition, albeit accompanied by a *significant reduction in reversibility* (as judged by the less steep gradient at low *q* and a small but discernible shift in the local minimum at high *q*; see lower set of three SAXS patterns shown in Figure 1a).

Notwithstanding the above qualitative observations, detailed SAXS analysis requires relatively low copolymer concentrations in order to avoid inter-particle interactions, which suppresses the scattering intensity at low *q*.<sup>2,3</sup> In practice, the scattering patterns can be satisfactorily fitted at a copolymer concentration of 1.0 % w/w using an established model<sup>4,5</sup> for worm-like micelles.

Figure 1b shows SAXS data obtained for 1.0 % w/w PLMA<sub>16</sub>-PBzMA<sub>37</sub> particles on heating from 20 to 160°C. At 20°C, the scattering pattern can be analyzed using a worm model<sup>4,5</sup>. Table 1 shows the key parameters obtained from the data fit using this model. Notably, the total worm cross-section is 15.4 nm and the worm contour length exceeds 600 nm, indicating highly anisotropic particles with a mean aspect ratio of more than 39, see Table 1. These values correlate well with our TEM observations. Another interesting observation is that these PLMA<sub>16</sub>-PBzMA<sub>37</sub> worms are relatively stiff, since their Kuhn length (160 nm) is an order of magnitude greater than the total worm cross-section. This is consistent with the bottle brush-like structure of the PLMA stabilizer block.

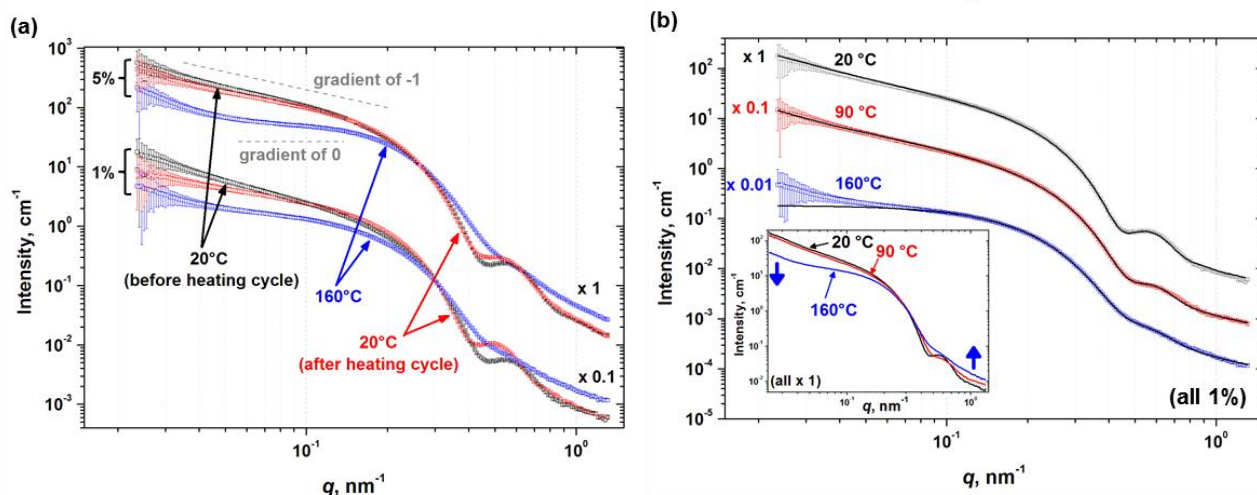


**Figure 1.** (a) Representative SAXS patterns for 5.0 and 1.0 % w/w PLMA<sub>16</sub>-PBzMA<sub>37</sub> copolymer dispersions in *n*-dodecane recorded during a 20°C - 160°C - 20°C thermal cycle. The 1.0 % w/w data is offset by a factor of 0.1 for clarity. Gradients of zero and negative unity (dashed grey lines) are also shown as a guide to the eye. (b) Representative SAXS patterns (symbols) for the same 1.0 % w/w PLMA<sub>16</sub>-PBzMA<sub>37</sub> copolymer dispersion in *n*-dodecane recorded during heating from 20°C to 160°C. In this case, SAXS patterns are offset a factor of 0.1 (90°C) and 0.01 (160°C) for clarity, fits to the data (solid lines) are shown and the results of this analysis are summarized in Table 1. The inset shows all three scattering patterns plotted on the same scale.

**Table 1. Structural parameters obtained from data fitting to SAXS patterns recorded for 1.0 % w/w PLMA<sub>16</sub>-PBzMA<sub>37</sub> diblock copolymer particles in *n*-dodecane at various temperatures: mean worm core cross-section ( $2R_{sw}$ ), total worm cross-section [ $2(R_{sw} + R_g)$ ], worm contour length ( $L_w$ ), aspect ratio [ $L_w/2(R_{sw} + R_g)$ ], worm Kuhn length ( $b_w$ ) and solvent fraction in the core of the particle ( $x_{sol}$ ).**

Temperature / °C	Mean worm core cross-section ( $2R_{sw}$ ) / nm	Total worm cross-section <sup>a</sup> [ $2(R_{sw} + R_g)$ ] / nm	Worm contour length ( $L_w$ ) / nm	Aspect ratio [ $L_w/2(R_{sw} + R_g)$ ]	Worm Kuhn length ( $b_w$ ) / nm	Solvent fraction in particle core <sup>c</sup> ( $x_{sol}$ )
20	12.8 ± 1.7	15.4 ± 1.8	>600 <sup>b</sup>	>39.0	160 ± 20	~0
90	12.0 ± 1.9	14.7 ± 2.0	350 ± 48	23.8 ± 6.5	143 ± 7	0.29
160	12.5 ± 2.8	15.1 ± 2.9	17.3 ± 0.5	1.15 ± 0.25	16.8 ± 1.7	0.48

<sup>a</sup>The radius of gyration of the PLMA corona block ( $R_g$ ) was found to be 1.3 nm in all cases. <sup>b</sup>The  $q$  range available for worm contour length analysis means that a reliable upper limit value cannot be calculated. <sup>c</sup>Uncertainties are smaller than the number of significant figures quoted.

## References:

- (1) Fielding, L. A.; Lane, J. A.; Derry, M. J.; Mykhaylyk, O. O.; Armes, S. P. *J. Am. Chem. Soc.* **2014**, *136*, 5790.
- (2) Garamus, V. M.; Pedersen, J. S.; Kawasaki, H.; Maeda, H. *Langmuir* **2000**, *16*, 6431.
- (3) Arleth, L.; Bergström, M.; Pedersen, J. S. *Langmuir* **2002**, *18*, 5343.
- (4) Pedersen, J. *J. Appl. Crystallogr.* **2000**, *33*, 637.
- (5) Pedersen, J. S.; Schurtenberger, P. *Macromolecules* **1996**, *29*, 7602.